Advances in Science and Technology Research Journal

Advances in Science and Technology Research Journal 2024, 18(5), 413–420
https://doi.org/10.12913/22998624/191313
ISSN 2299-8624, License CC-BY 4.0

Received: 2024.06.28
Accepted: 2024.07.20
Published: 2024.08.01

Investigation of Sodium Hydroxide on the Electrolysis and Silica based Nano Fluid on the Performance of Proton Exchange Membrane Fuel Cell

Addala Satyanarayana[1*], I.E.S. Naidu[1]

[1] Department of EECE, Gitam Deemed to be University, Vizag, A.P, India

* Corresponding author e-mail: addalasatyam@gmail.com

ABSTRACT

Energy efficiency is a global need to decrease net emissions and optimise the use of renewable energy sources. Ongoing research focuses on optimizing the use of renewable energy resources to maximize their consumption. Fuel cells, which utilise water to generate electricity, are among these renewable energy resources. Nevertheless, as previously said, there is ongoing research focused on optimising the synthesis of hydrogen and the extraction of voltage and current. In this study, we present the utilisation of sodium hydroxide (NaOH) in the extraction of hydrogen and silica nanoparticles for the enhancement of power values. The experiment clearly demonstrates that using a 50% NaOH solution resulted in the production of about 5.602 litres of hydrogen gas. Furthermore, the molar percentage of hydrogen in the final product was determined to be 85.74%. The gas chromatography analysis findings indicate that the product contains 81.58% hydrogen, 11.62% nitrogen, and 0.04% carbon dioxide. The electrical efficiency achieved is 86% with a heat loss of 13.96%. In addition, the research included the introduction of silica nanoparticles into the water. It was noted that this led to an increase in power density when the relative humidity was about 70%. The study also revealed that these nanoparticles had the potential to boost fuel cell performance.

Keywords: fuel cell, sodium hydroxide, electrolysis, silica nanoparticles, relative humidity, power density.

INTRODUCTION

As a consequence of the rising diversity of the world's population, there is a mismatch between the production of energy and the use of energy over the whole planet. Because of the simplicity with which these resources may be accessed and the decreased cost of these resources, there has been a dramatic rise in the utilisation of energy resources that are based on fossil fuels. This is due to the fact that fossil fuels are more readily available. Renewable energy sources are used as alternatives to conventional energy resources with the objective of reducing the use of fossil fuels and making a substantial contribution to the achievement of net zero emissions [1–3]. Although they were first developed in the 18th century, fuel cells have since found widespread use in a variety of stationary installations [4]. In compared to other types of energy converters, a proton exchange membrane fuel cell (PEMFC) is a kind of fuel cell that generates cleaner energy by using the electrochemical process that occurs between hydrogen and oxygen. The proton exchange membrane fuel cell is commonly considered to be a highly promising energy converter due to the major benefits it has in comparison to other devices that are now available within the market [5–6]. The power density of a PEMFC is higher than that of traditional fuel cells, and its actual efficiencies may reach up to sixty percent higher than that of conventional fuel cells. PEMFCs are not complete without the proton exchange membrane (PEM), which is an essential component. In addition to maintaining a barrier between the anode and the cathode, it makes it easier for protons to go from the anode to the cathode. Strong mechanical qualities, great electrochemical efficiency, and outstanding

temperature and chemical stability are all requirements for the PEM for it to be considered suitable. Recent studies have been conducted with the objective of accelerating the commercialization of fuel cells. These studies are centred on the achievement of higher electrochemical performance at low temperatures and humidity, while also taking into consideration the operating temperature of fuel cells. In light of this, in order to preserve the following: According to the information presented above, metal oxides have been used in a number of scientific activities in order to create channels for proton transfer. This has been done in order to maintain the membrane's moisture level in the event that the temperature or humidity conditions are low. When the sulfonated metal oxide is functionalized, it has the potential to serve as a vehicle owing to the existence of a proton transfer channel and the intrinsic negative charge that it has. As a consequence, it is anticipated that considerable effects would occur [7–8]. Over the last several years, there has been a substantial rise in the utilisation of nanofluid systems in applications that include more than one device. In terms of their fundamental examination, a large number of studies have been completed and published. In the current day, researchers are focusing their attention on the thermal application of nanofluids because of the nanofluid system's promising behaviour in terms of enhancing thermal conductivity. All of these studies have been completed and published. Nanofluid systems, on the other hand, are especially convincing in applications that contain non-conventional energy sources, such as fuel cells, and photovoltaic instruments. These are all examples of applications that may benefit from their use [9–12].

Nevertheless, research in the nanofluid sector has also focused on using nanofluid in other devices, including heat exchangers. This is due to the extensive efforts made by researchers to enhance the performance of such devices, aiming to address the global energy demand and mitigate the issue of fossil fuel depletion [13–14]. Due to the advantageous impact of fuel cells compared to alternative power generators like internal combustion (IC) engines and batteries, the utilisation of fuel cells has grown more widespread in contemporary times [15–16]. Fuel cells are the electrochemical devices that can convert chemical energy into electrical energy, unlike combustion engines and batteries. In addition, fuel cells have the ability to generate higher amounts of electrical energy while functioning at lower temperatures. In addition to compounding the negative impact, fuel cell devices possess the advantageous characteristics of being more compact, having less mass, and generating lower levels of noise, increased productivity and extended lifespan.

In a study conducted by Günestekin et al. [17], the researchers examined the impact of nanocatalyst, carbon nanotubes, and hybrid graphene quantum dots-carbon nanotubes on the current signal of methanol fuel cell (DMFC) devices. According to the findings of the inquiry, the hybrid graphene quantum dots-carbon nanotubes nanocatalyst exhibited the maximum performance in terms of current density when compared to other nano-catalysts. By using metal carbides and/or nitrides (MXene) nanoparticles coupled with platinum ruthenium catalyst to produce a new electro-catalyst, Abdullah et al. [18] were able to optimise the performance of a DMFC system. In the course of the study project, it was discovered that the current density of nano enhanced catalyst is about 2.34 times greater than that of catalyst that is utilised in commercial applications. The authors come to the conclusion that the extraordinary morphology of MXene, which is capable of facilitating a more rapid transfer of ions, is responsible for the enhancement in electrocatalyst performance. Pourfayaz et al. [19] did a research on a combined polymer electrolyte membrane fuel cell and absorption chiller system. This chiller used several types of nanofluids, including silver (Ag) nanoparticles-water nanofluid, and aluminium oxide nanoparticles-water nanofluid, as coolants. The objective was to improve the coefficient of efficiency of the whole system. The research determined that the refrigerant, which included a dispersion of silver nanoparticles, attained an overall efficiency of 81%. In a separate study, Kordi et al. [20] used a numerical method to examine the efficiency of a fuel cell with a polymer electrolyte membrane. The fuel cell was aided by the use of aluminium oxide nanoparticles-water nanofluid as a cooling agent. The study included dispersing aluminium oxide nanoparticles in varying volume concentrations within the base fluid to examine the impact of nano additive volume concentration on the cooling rate of a four-plate cooler. The numerical analysis revealed that the use of nanofluid accelerated the cooling process and greatly improved the fuel cell's efficiency. Specifically, the use of a nanofluid with a volume concentration of 0.006% brought about

a decrease of 13% in the temperature uniformity index, along with an increase of 35% in pressure drop. The findings imply that the inclusion of nanofluids in cooling plate devices could enhance heat transfer characteristics, resulting in enhanced fuel cell performance. In their study, Zakaria et al. [21] examined the use of nanofluid coolants containing Al_2O_3 particles distributed in water and water/ethylene glycol solutions for cooling PEM fuel cells. The nanoparticles were limited to a maximum volume percentage of just 0.5%v due to the significant increase in electrical conductivity that occurred with higher percentages. An additional ratio was established to measure the proportional growth of both thermal and electrical conductivity. As a result, it is clear from the research that has been shown above that nanoparticles have the potential to be used in fuel cells for the purpose of cooling the fuel cell and extracting hydrogen while it is functioning.

The generation of hydrogen is one of the most significant parts of the fuel cell, which is performed by the electrolysis process with the help of metal electrodes. For example, the dispersion of metal may be enhanced by using materials such as Al_2O_3, SiO_2, carbon nanotubes [22], CeO_2 [23], and graphene [24]. Hydrogen originates mostly from water, and the hydrogen that is produced can be used for the generation of energy as well as the engines of vehicles because it is simple to convert and is beneficial to the environment. The use of this kind of energy is preferred for traditional vehicles as a fuel because it decreases the amount of carbon monoxide that is released and contributes to the achievement of net zero emissions. In addition to being a renewable source of energy, this particular form of energy discharges heat energy during the process of hydrogen extraction. Electrolysis of water is considered the most efficient method for hydrogen production. This process involves the decomposition of water into oxygen and hydrogen gas using an electric current. During the reaction occurring at the cathode, two water molecules capture two electrons, resulting in the production of hydrogen gas (H_2) and hydroxide ions (OH^-). Meanwhile, at the anode, two additional water molecules undergo decomposition to produce oxygen gas (O_2), releasing 4H+ ions and transferring electrons to the cathode. The H^+ and OH^- ions undergo neutralisation, resulting in the formation of water molecules. The overall reaction for the electrolysis of water can be represented as:

$$2H_2O(l) \rightarrow H_2(g) + O_2(g)$$

Hydrogen and oxygen gas emanate from this reaction and form bubbles at the electrode, which can be collected. This principle is employed for the manufacture of hydrogen and hydrogen peroxide, leading to the generation of hydrogen vehicle fuel. For this investigation, we evaluated the hydrogen (H_2) productivity generated by comparing the total volume, production rate, and production time of hydrogen created through the electrolysis process using different concentrations of sodium hydroxide (NaOH) as the catalyst.

MATERIALS AND METHODS

Every component used in the production of silica nanoparticles was of high quality and readily available, requiring no additional purification. An initial component, tetraethyl orthosilicate (TEOS) ($SiC_8H_{20}O_4$, Sigma Aldrich), was employed in the sol-gel synthesis technique. In addition, ethanol (C_2H_5OH, GK Life Sciences) and hydrochloric acid (HCl, SRL Chemicals ltd.) were used as part of the procedure. The initial step of the synthesis process involved adding 10 ml of ethanol to a clean beaker and stirring it on a magnetic stirrer at a speed of 500 rpm. Next, a small amount of hydrochloric acid was carefully added to the mixture while it was being stirred consistently. After some time, 1.5 ml of tetraethyl orthosilicate (TEOS) were added and stirred for about 15 minutes. The solution that was produced underwent a process of drying in a hot air oven at 150 °C for four hours, followed by annealing in a muffle furnace at 300 °C for five hours to obtain the desired silica nanoparticles. Each of these processes occurred within a span of twenty-four hours.

RESULTS AND DISCUSSION

The crystal structure and functional bond analysis of the silica nanoparticles were studied using X-ray and Fourier transformation infrared spectroscopy (FTIR) respectively and presented in Figure 1a and Figure 1b. Based on the given diffraction pattern 1a, the Debye-Scherer Equation can be used to calculate the crystallite size of the silica nanoparticles. The Equation is:

$$D = K\lambda / (\beta * cos\theta) \quad (1)$$

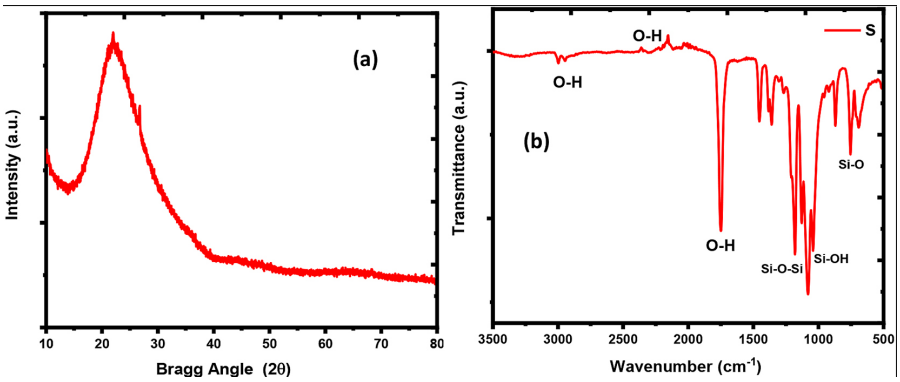

Figure 1. XRD (a) and FTIR (b) spectra of silica nanoparticles

This Equation 1 describes the connection between various parameters within the context of crystallites. “D” denotes the average size of the crystallites, while a constant ”K” (0.9) is used to represent the relationship with the crystallite size. The wavelength of the employed X-ray is represented by ”λ” (1.54), and the full width at half maximum (FWHM) is denoted by ”β”. Lastly, the Bragg angle is represented by ”θ”. Figure 1a shows a significant peak in the X-ray spectrum at a Bragg angle of 22°, indicating the possible existence of silica nanoparticles that reflect from the (100) plane. This observation is consistent with previous research [25, 26]. The XRD pattern indicates that the silica nanoparticles have a hexagonal crystal structure and display primitive lattices with parameters a = b = 4.913 A° and c = 5.405 A°. According to the Debye Scherer formula, the crystallite size of the silica nanoparticles, following calcination at 300 °C, measures approximately 48 nanometers. This discovery highlights the amorphous nature of the nanoparticles and their incredibly small size, resulting in a strong connection between silicon (Si) and oxygen (O). Figure 1b displays the FTIR spectra of the silica nanoparticles synthesised through the sol-gel method. The analysis was performed using Origin pro. The vibration frequencies at 2976 cm^{-1}, 1656 cm^{-1}, and 2122 cm^{-1} confirm the presence of hydroxyl O-H bonds in the silica nanoparticles. Furthermore, the appearance of peaks at 1126 cm^{-1}, 1056 cm^{-1}, and 746 cm^{-1} suggests the formation of Si-O-Si, Si-OH, and Si-O, respectively. These findings align with prior studies that have been published [27, 28].

The field emission scanning electron microscopy FESEM image of the colloidal suspension (sol) and gelation to form a system in continuous liquid phase (gel) sol-gel synthesised silica nanoparticles is shown in Figure 2a, accompanied by the elemental analysis in Figure 2b conducted through Energy dispersive X-ray analysis.

Figure 2a clearly illustrates the formation of silica flakes measuring approximately 500 nm in size. The weight percentage of silicon is 56.7, while oxygen accounts for 43.3%. The particles were gradually injected into the hydrolysis chamber while undergoing hydrolysis in order to assess the effectiveness of silica nanoparticles in enhancing hydrogen extraction and cell voltage extraction. The data on hydrogen generation was obtained by measuring the change in water level

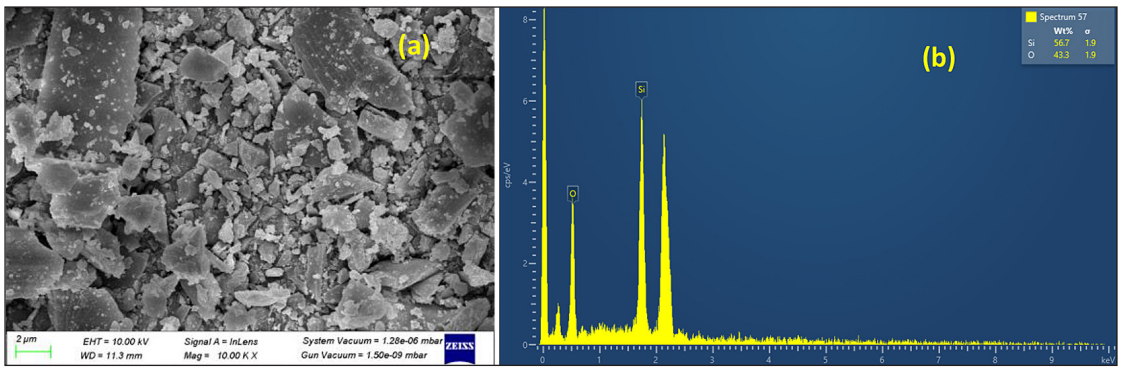

Figure 2. FESEM image (a) and energy dispersive X-ray (EDAX) spectra (b) of silica nanoparticles

in the measuring tube before and after the electrolysis process. This was done using different concentrations of NaOH and during a certain time period. The disparity in water level in the measuring tube was then used to ascertain the amount of seawater before to and subsequent to the electrolysis process, which indicated the volume of hydrogen generated by the electrolysis process. Moreover, this hydrogen volume data was then used to compute the production rate and yield of hydrogen, as well as the yield of hydrogen generated by the electrolysis process of saltwater extracted from a mangrove plantation region, using different concentrations of NaOH as a catalyst. The study findings were processed and discussed using quantitative descriptive analysis.

For this investigation, an electrode made of stainless steel was utilised in the electrolysis procedure. Applying a direct voltage between the two electrodes creates an electric potential difference. When a potential difference is present, ions in the electrolyte solution are attracted to the electrode with the opposite charge. The ions observed in this investigation are a result of the dissociation of NaOH, just as a materials scientist would expect. When the NaOH solution dissociates, it forms Na^+ and OH- ions. Within the electrolyte solution, the positively charged sodium (Na^+) and hydrogen (H^+) ions are drawn towards the cathode, while the negatively charged hydroxyl (OH^-) ions are directed towards the anode. Just at the electrode, a redox reaction occurs due to the movement of these ions, resulting in the creation of an electric current in the solution. Figure 3 demonstrates the relationship between the concentration of NaOH used in the electrolysis of hydrogen water and the corresponding increase in the amount of water used as the raw material. Water is filled in the storage tube to facilitate the electrolysis process for the hydrogen (H_2) and oxygen (O_2) gas. After the initial 20 min of electrolysis, gas will start to build up in the reservoir tube. Based on the measurements taken during the procedure, it has been observed that hydrogen gas begins to appear around the 20th second. Through this experiment, it is evident that as the quantity of hydrogen gas increases, the water level decreases. By applying the cylindrical volume equation to the gas height data in the tube, it is possible to determine the gas level and calculate the amount of gas produced. The concentration of the NaOH solution directly affects the amount of hydrogen gas produced, as indicated in the literature review. Figure 3 presents data illustrating the correlation between the concentration of NaOH solution and the quantity of hydrogen gas produced.

The data collection method involved conducting five tests, with each test using a distinct concentration of the NaOH solution: 10%, 20%, 30%, 40%, and 50%. Based on the experimental results, it is evident that there is a clear relationship between the concentration of the sodium hydroxide (NaOH) solution and the quantity of hydrogen (H_2) gas produced. During the initial experiment with a 10% NaOH solution, the volume of hydrogen gas generated amounted to 3.2901 litres. In the subsequent trial, the volume of hydrogen gas expanded to 4.0861 litres. The increase in hydrogen volume is quite small, measuring approximately 0.8 litres. In the following iteration, there is an increase in the volume of hydrogen gas by approximately 0.1 l. The production of hydrogen gas is still increasing from the previous run, although the rate of increase is not as high as in the first and second runs. The NaOH solution is effective as an electrolyte in this process. Based on conducted research, it has been found that the use of electrolytes containing sodium (Na) can lead to the formation of visible flocs in gas storage tubes. Obstructions in the electrode pipeline can impede the reaction and hinder the breakdown of water into hydrogen and oxygen.

By examining the production of hydrogen gas in a laboratory experiment and conducting a literature study, it becomes clear that there are discrepancies in the results. Just like a physicist, the data from the literature study revealed a clear linear relationship as the volume increased. However, the experimental results took a different

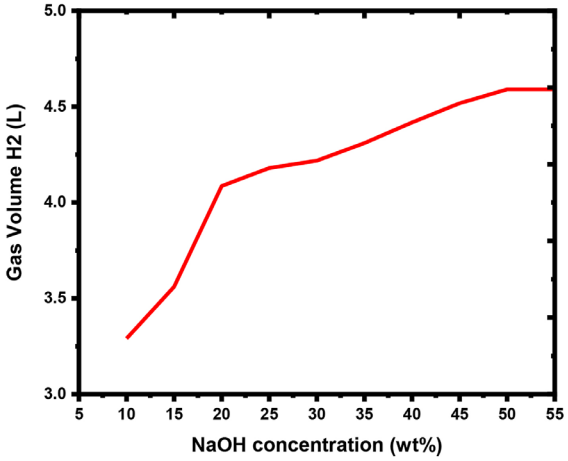

Figure 3. Experimental study on effect of sodium hydroxide electrolyte solution concentration to the volume of hydrogen gas production

path, showing a tendency to decrease instead. Based on the literature review, the highest quantity of hydrogen that can be generated is 24.4786 litres. In addition, Figure 3 shows that the largest amount of hydrogen is 4.5902 litres. There is a clear distinction that occurs. Based on scientific principles, it can be deduced that when the concentration reaches 10%, the volume of hydrogen should ideally be 5.8869 litres. However, in reality, the volume of hydrogen is only 3.2901 litres. The difference is negligible since the electrode pipe is still functioning properly and remains free from contamination.

In the second experiment result, there is a slight difference observed at a 20% NaOH concentration. The calculated value is 11.6752 litres, whereas the measured value is 4.0861 litres. It became evident that there was a noticeable difference between the expected and observed outcomes during the fifth trial, particularly when utilising a 50% NaOH solution. According to the calculations, the theoretical results come out to be 24.7486 litres, while the experimental results show 4.5902 litres. There is a difference of about 20 litres. The decrease in the volume of hydrogen by up to 20 litres in the experiment can be explained by a decline in the electrode's performance, which is becoming more saturated.

The theoretical equilibrium voltage for water electrolysis is 9.08 Volts. Analysis of NaOH concentration yields potential cell values from 12.04 to 12.07 Volts. Note that this electrolysis process needs a voltage significantly greater than equilibrium. The experiment tool panel sets the voltage as 13.1 Volts, but it's really 13.3 Volts. The system has a continuous over potential since the equilibrium voltage of 9.08 V is measured in an unreachable standard state. Over potential raises working voltage much above equilibrium. The source voltage may be changed to enhance the working voltage while maintaining current. The minimal voltage needed for consistent beginning current is called the working voltage. The actual cell potential value exceeds the predicted cell potential limit, showing that each reaction and concentration variation may be satisfied.

The temperature variation with proton conductivity was demonstrated in Figure 4 with various concentrations of silica nanoparticles.

The silicon dioxide (SiO_2) membrane's water absorption and volume swelling are strongly connected to proton exchange membranes' water interaction. Water absorption is the membrane's

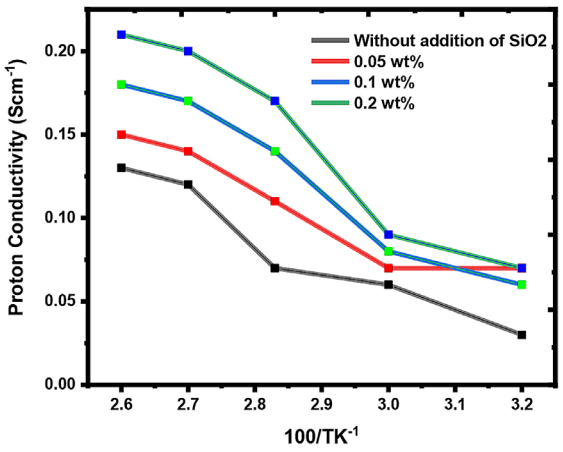

Figure 4. Graph depicting the variation of proton conductivity with temperature

capacity to absorb water in water. Water molecules are essential for proton conduction in fuel cells, hence proton exchange membranes must maintain water. Proton exchange membranes expand after water absorption. The mechanical strength of the proton exchange membrane may be reduced by excessive swelling, compromising fuel cell stability and longevity. Comparison shows that silicon dioxide (SiO_2)-nanoparticle membrane absorbs more water than pure Nafion membrane(sulfonated tetrafluoroethylene based fluoropolymer-copolyme). Silica's porous structure, surface area, and adsorption capability help the proton exchange membrane retain water.

CONCLUSIONS

Silica nanoparticles were synthesized using sol-gel synthesis in a rapid way to study their effect on the proton conductivity. NaOH was used as the catalyst to boost the electrolysis process using water. XRD investigations on the silica nanoparticles evidenced the amorphous nature of silica. FTIR investigations on the silica nanoparticles identified the formation of silica functional bonds and was also supported by EDAX analysis. FESEM investigations endorsed the formation of flake-like structures in the as-synthesized silica nanoparticles. Further, the addition of silica nanoparticles into the host liquid i.e., water improved the proton conductivity and water absorption. The electrolysis process yields a significant volume of hydrogen gas, reaching 4.5902 litres. Thus, the ideal NaOH concentration in this study is 50%.

REFERENCES

1. Gayen D., Chatterjee R. Roy S. A review on environmental impacts of renewable energy for sustainable development. Int. J. Environ. Sci. Technol. 2024; 21: 5285–5310. https://doi.org/10.1007/s13762-023-05380-z
2. Wilberforce T., Olabi A., Sayed E.T., Mahmoud M., Alami A.H., Abdelkareem M.A. The state of renewable energy source envelopes in urban areas. International Journal of Thermofluids, 2024; 21: 100581. https://doi.org/10.1016/j.ijft.2024.100581
3. Husain A.M., Hasan M.M., Khan Z.A., Asjad M. A robust decision-making approach for the selection of an optimal renewable energy source in India. Energy Conversion and Management, 2024; 301 117989. https://doi.org/10.1016/j.enconman.2023.117989
4. Manoo M.U., Shaikh F., Kumar L., Arıcı M. Comparative techno-economic analysis of various standalone and grid connected (solar/wind/fuel cell) renewable energy systems. International Journal of Hydrogen Energy, 2024; 52: 397–414. https://doi.org/10.1016/j.ijhydene.2023.05.258
5. Hou X., Sun R., Huang J., Geng W., Li X., Wang L., Zhang X. Energy, economic, and environmental analysis: A study of operational strategies for combined heat and power system based on PEM fuel cell in the East China region. Renewable Energy, 2024; 223: 120023. https://doi.org/10.1016/j.renene.2024.120023
6. Asghar R., Hassan S., Yaqoob Y. A comprehensive overview of wet chemistry methodologies and their application in the fabrication of materials for PEM fuel cell. International Journal of Hydrogen Energy, 2024; 58: 1190–1203. https://doi.org/10.1016/j.ijhydene.2024.01.289
7. Aigbe U.O., Osibote O.A. Green synthesis of metal oxide nanoparticles, and their various applications. Journal of Hazardous Materials Advances, 2024; 13: 100401. https://doi.org/10.1016/j.hazadv.2024.100401
8. Jamalpour S., Shamsabadi A., Arab K., Tohidian M., Tamsilian Y., Hooshyari K., Rahmani S. Two-dimensional nanomaterials-based polymer nanocomposites for fuel cell applications, 2024; 465–508. https://doi.org/10.1002/9781119905110.ch13
9. Akram M., Rani M., Shafique R., Batool K., Habila M.A., Sillanpää M. Fabrication of $LaCrO_3$@ SiO_2 nanoparticles supported with graphene-oxide for capacitive energy storage and photocatalytic degradation applications. J Inorg Organomet Polym, 2024; 34: 361–373. https://doi.org/10.1007/s10904-023-02814-6
10. Zheng C., Xie N., Liu X., Wang L., Zhu W., Pei Y., Yue R., Liu H., Yin S., Yao J., Zhang J., Yin Y., Guiver M.D. Durability improvement of proton exchange membrane fuel cells by doping silica–ferrocyanide antioxidant. Journal of Membrane Science, 2024; 690, 122195. https://doi.org/10.1016/j.memsci.2023.122195
11. Wu D., Ren H., Huang X., Ge W., Xie T., Tian Z., Meng F., Lin H., Li H. Strengthening functional properties and competitive crystallization behavior of La_2O_3-BaO-CaO-Al_2O_3-B_2O_3-SiO_2 glass-ceramic for solid oxide fuel cells: Agglomeration effect of rare-earth oxide. Journal of Non-Crystalline Solids, 2024; 632: 122933. https://doi.org/10.1016/j.jnoncrysol.2024.122933
12. Saeed M., Marwani H.M., Shahzad U., Asiri A.M., Rahman M.M. Nanoscale silicon porous materials for efficient hydrogen storage application. Journal of Energy Storage, 2024; 81: 110418. https://doi.org/10.1016/j.est.2024.110418
13. Hussein A.K., Rashid F.L., Rasul M.K., Basem A., Younis O., Homod R.Z., El Hadi Attia M., Al-Obaidi M.A., Ben Hamida M.B., Ali B., Abdulameer S.F. A review of the application of hybrid nanofluids in solar still energy systems and guidelines for future prospects. Solar Energy, 2024; 272: 112485. https://doi.org/10.1016/j.solener.2024.112485
14. Soudagar M.E.M., Shelare S., Marghade D., Belkhode P., Nur-E-Alam M., Kiong T.S., Ramesh S., Rajabi A., Venu H., Yunus Khan T., Mujtaba M., Shahapurkar K., Kalam M., Fattah I. Optimizing IC engine efficiency: A comprehensive review on biodiesel, nanofluid, and the role of artificial intelligence and machine learning. Energy Conversion and Management, 2024; 307: 118337. https://doi.org/10.1016/j.enconman.2024.118337
15. Kendall K., Ye S., Liu Z. The hydrogen fuel cell battery: Replacing the combustion engine in heavy vehicles. Engineering, 2023; 21: 39–41. https://doi.org/10.1016/j.eng.2022.11.007
16. Fan L., Tu Z., Chan S.H. Recent development of hydrogen and fuel cell technologies: A review. Energy Reports, 2021; 7: 8421–8446. https://doi.org/10.1016/j.egyr.2021.08.003
17. Günes B.G., Tekin H. Medetalibeyoglu N., Atar, M. Lütfi Yola. Efficient directmethanol fuel cell based on graphene quantum dots/multi-walled carbon nanotubes composite, Electroanalysis 2020; 321977–1982.
18. Abdullah N., Saidur R., Zainoodin A.M., Aslfattahi N. Optimization of electrocatalyst performance of platinum–ruthenium induced with MXene by response surface methodology for clean energy application, J. Clean. Prod. 277 (2020/12/20/2020) 123395.
19. Pourfayaz F., Imani M., Mehrpooya M., Shirmohammadi R. Process development and exergy analysis of a novel hybrid fuel cell-absorption refrigeration system utilizing nanofluid as the absorbent liquid, Int. J. Refrig. 2019; 97: 31–41.

20. Kordi M.A.J. Afshari M.E. Effects of cooling passages and nanofluid coolant on thermal performance of polymer electrolyte membrane fuel cells, Journal of Electrochemical Energy Conversion and Storage 2019; 16(3): 031001.
21. Zakaria I., Mohamed W., Azid N., Suhaimi M., Azmi W. Heat transfer and electrical discharge of hybrid nanofluid coolants in a fuel cell cooling channel application. Applied Thermal Engineering, 2022; 210: 118369. https://doi.org/10.1016/j.applthermaleng.2022.118369
22. İzgi M.S., Baytar O., Şahin Ö., Kazıcı H.Ç. CeO_2 supported multimetallic nano materials as an efficient catalyst for hydrogen generation from the hydrolysis of $NaBH_4$. International Journal of Hydrogen Energy, 2020; 45(60): 34857–34866. https://doi.org/10.1016/j.ijhydene.2020.04.034
23. Yao Q.L, Lu Z.H., Jia Y.S., Chen X.S., Liu X. In situ facile synthesis of Rh nanoparticles supported on carbon nanotubes as highly active catalysts for H-2 generation from NH3BH3 hydrolysis. Int J Hydrogen Energy 2015; 40: 2207e15.
24. Alekseeva O.K., Pushkareva I.V., Pushkarev A.S., Fateev V.N. Graphene and graphene-like materials for hydrogen energy. Nanotechnol Russia, 2020; 15: 273–300. https://doi.org/10.1134/S1995078020030027
25. Sharma P., Kherb J., Prakash J., Kaushal R. A novel and facile green synthesis of SiO_2 nanoparticles for removal of toxic water pollutants. Appl Nanosci. 2023; 13(1): 735–747. https://doi.org/10.1007/s13204-021-01898-1
26. Duraisamy N.K., Periakaruppan R., Abed S.A., Al-Dayan N., Dhanasekaran S., Aldhayan S.H.A. Production and characterization of Azadirachta indica-mediated SiO_2 nanoparticles and an evaluation of their antioxidant and antimicrobial activities. Silicon. 2023; 15(15): 6663–6671. https://doi.org/10.1007/s12633-023-02544-x
27. Ece M.Ş., Ekinci A., Kutluay S., Şahin Ö., Horoz S. Facile synthesis and comprehensive characterization of Ni-decorated amine groups-immobilized Fe_3O_4@SiO_2 magnetic nanoparticles having enhanced solar cell efficiency. J Mater Sci Mater Electron. 2021; 32(13): 18192–18204. https://doi.org/10.1007/s10854-021-06361-z
28. Choi M., Choi W.K., Jung C.H., Kim S.B. The surface modification and characterization of SiO_2 nanoparticles for higher foam stability. Sci Rep. 2020; 10(1): 19399. https://doi.org/10.1038/s41598-020-76464-w
29. Saputro R.A and Rangkuti Ch. Pengaruh molaritas larutan cairan elektrolit dan arus listrik terhadap Gas HHO yang Dihasilkan Pada Generator HHO Tipe Dry Cell. 4h National Scholar Seminar, Trisakti University, 2018.